Conference Proceedings

Solar World Congress 2015
Daegu, Korea, 08 – 12 November 2015

The dynamic performance of different configurations of Solar Aided Power Generation (SAPG)

Jiyun Qin, Eric Hu, Graham J. Nathan

School of Mechanical Engineering, the University of Adelaide, Adelaide (Australia)

Abstract

Solar Aided Power Generation (SAPG) is defined as solar heat used to displace extraction steam to preheat the regenerative Rankine cycle (RRC) power plant's feedwater. In an SAPG plant, heat exchangers (termed as solar preheaters, SP) facilitate the heat exchange between solar heat and feedwater. Depending on the locations of the SPs in the power plant, an SAPG plant can have different configurations. In order to respond to solar variations, SAPG plants can be controlled using different approaches. The performance of SAPG plants with different configurations and controlled using a different approach has been compared by using real solar radiation data from Adelaide, Australia. Solar radiation data from two consecutive periods of five days during summer and winter were used for simulation. The results show that the performances of the SAPG plant with different configurations and approaches to control are different, and there is an optimum configuration and approach to control for the SAPG plant.

Keywords: *Solar Aided Power Generation, Plant configurations, Series configuration, Parallel configuration, Dynamic performance.*

1. Introduction

A Solar Aided Power Generation (SAPG) plant is a variant of the regenerative Rankine cycle (RRC) power plant. In an RRC power plant, steam is extracted from the steam turbine to preheat the feedwater in a feedwater heater (FWH). In an SAPG plant, solar thermal energy carried by the heat transfer fluid (HTF) is used to displace the heat of the extraction steam by preheating the feedwater. The displaced extraction steam can be expanded further to produce power. Compared with solar-only power plants, an SAPG plant has advantages of lower cost and higher solar to power efficiency (Hu et al., 2010).

In an SAPG plant, a heat exchanger (called a solar preheater, SP) is used to facilitate the heat exchange between the solar thermal energy and heat of the feedwater. The heat exchanger can be arranged in parallel or series with the FWHs. Most of previous studies about the SAPG plant are based on the configurations that the SP is in parallel with the FWHs of power plants (Yan et al., 2010; Yang et al., 2011; Peng et al., 2013, 2014a, 2014b; Hou et al., 2015). In contrast, some recent studies about the SAPG plant are based on the configuration that the SP is in series with the FWHs (Hou et al., 2013; Wu et al., 2015). Based on the steady state simulation, Yan et al. (2010) and Yang et al. (2011) found that more solar input leads to higher technical performance. Peng et al. (2013, 2014a, 2014b) assessed an SAPG plant by using daily solar radiation data from different seasons. It was found that the efficiency of the solar field is influenced by the variations in solar radiation. Hou et al. (2013, 2015) and Wu et al. (2015) evaluated SAPG plant performance by using annual solar radiation data. Hou et al. (2013) assessed an SAPG plant without any solar storage system while Wu et al. (2015) assessed an SAPG plant with a solar storage system. It is found that the performance of the SAPG plant is influenced by the solar radiation. However, these previous studies about the SAPG plant are based on the single configuration. The comparison between different configurations is

doi:10.18086/swc.2015.04.17 Available at http://proceedings.ises.org

lack of study.

In order to respond to solar variability, the extraction steam of an SAPG plant can be controlled with different approaches. Hou et al. (2013, 2015) and Wu et al. (2015) evaluated the SAPG plant based on an assumption that feedwater outlet temperature of FWHs keeps unchanged. This means that all the extraction steam should be adjusted in response to solar resources. However, the SAPG plant can also be controlled with varying feedwater outlet temperature of FWHs. This means that the extraction steam can be adjusted in pre-set order to respond to solar resource variability. This may help to improve the performances of the SAPG plant.

Hou et al. (2013) evaluated SAPG performance by using real solar radiation data. The result showed that the performance of an SAPG plant is influenced by the solar radiation. However, the SAPG plant in the papers of Hou (2013) and Peng (2013, 2014a, 2014b) are based on the parallel configuration. It is necessary to compare the dynamic performance of four configurations controlled using different approaches under variations of solar radiation.

2. Concept description

Depending on the locations of Solar Preheaters, an SAPG plant can have four different configurations, termed as Parallel 1 (P1), Parallel 2 (P2), Series 1 (S1) and Series 2 (S2) configurations. Figures 1 to 4 shows the schematic diagram of P1, P2, S1 and S2 configurations, respectively. As shown in Fig. 1 and 2, in the P1 the P2 configurations the SP is parallel with the FWHs of the power plant. In the P1 configuration, each FWH has one parallel SP, while in the P2 configuration, all the high pressure FWHs or low pressure FWHs have one parallel SP. As shown in Fig. 3 and Fig. 4, in the S1 and the S2 configurations the SP is in series with the FWHs of the power plant. In the S1 configuration, the SP is located in series between FWH3 and DEA (deaerator) to displace the extraction steam before the extraction point at DEA (points A, B and C in Fig. 3), or is located in series between FWH8 and the condenser to displace the extraction steam after the extraction point at DEA (points D to H in Fig. 3). In the S2 configuration, the SP is located in series between the boiler and FWH1 to displace the extraction steam before the extraction point at DEA (points A, B and C in Fig. 4), or is located in series between DEA and FWH5 to displace the extraction steam after the extraction point at DEA (points D to H in Fig. 4). In the S1 configuration, the extraction steam is displaced from lower pressure extraction points to higher pressure extraction points; while in the S2 configuration, the extraction steam is displaced from higher pressure extraction points to lower pressure extraction points.

In order to respond to solar variability, the SAPG plant can be controlled with two typical approaches: (1) at a constant feedwater temperature exiting FWH (CT); or (2) at a varying feedwater temperature exiting FWH (VT). The CT approach means that the outlet temperature at each FWH is maintained as constant by adjusting the extraction steam flow rates at all designated displaced extraction points (i.e. points A to C or E to H in Figs. 1 to 4). The VT approach means that the extraction steam flow rate at the designated displaced extraction points (i.e. points A to C or E to H in Figs. 1 to 4) is displaced in pre-set order to respond to solar resource variability. In the VT approach, the two most typical pre-set orders are: (1) the extraction steam is displaced in order from higher pressure extraction point to lower pressure extraction point, which is termed as the HL-VT approach; or (2) the extraction steam is displaced in order from the lower pressure extraction point to the higher pressure extraction point, which is termed as the LH-VT approach. Different configurations can be controlled with different approaches in response to solar variability. Table 1 summarises the configurations and their possible control approaches.

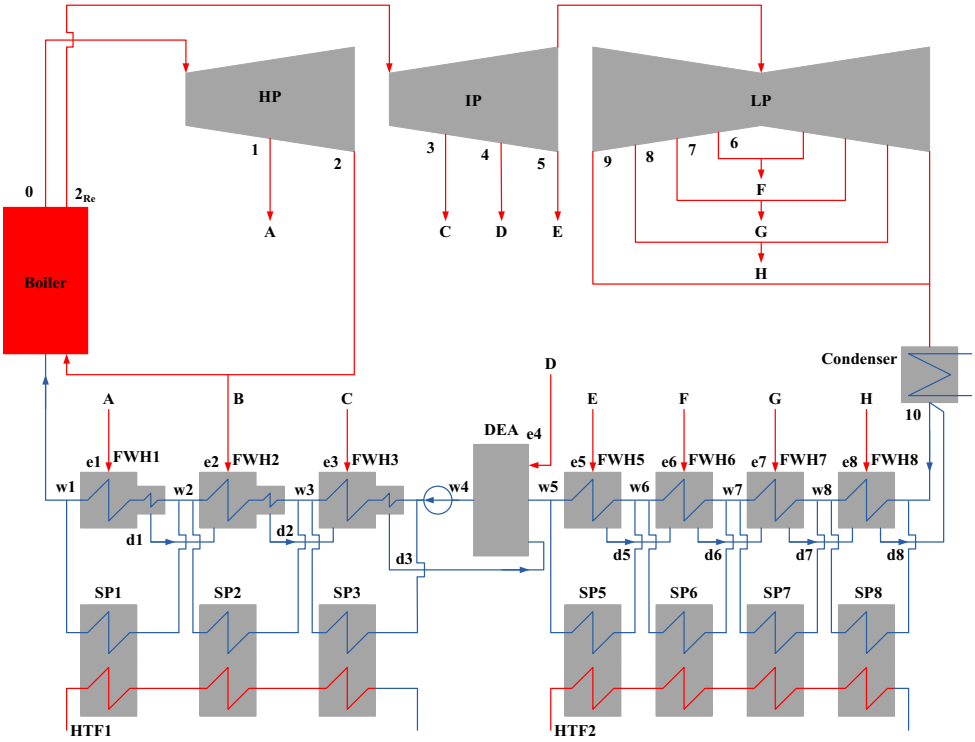

Fig. 1: Schematic diagram of a Parallel 1 (P1) SAPG plant, HTF 1 is used to displace the extraction steam at points A to C and HTF2 is used to displace the extraction steam at points E to H.

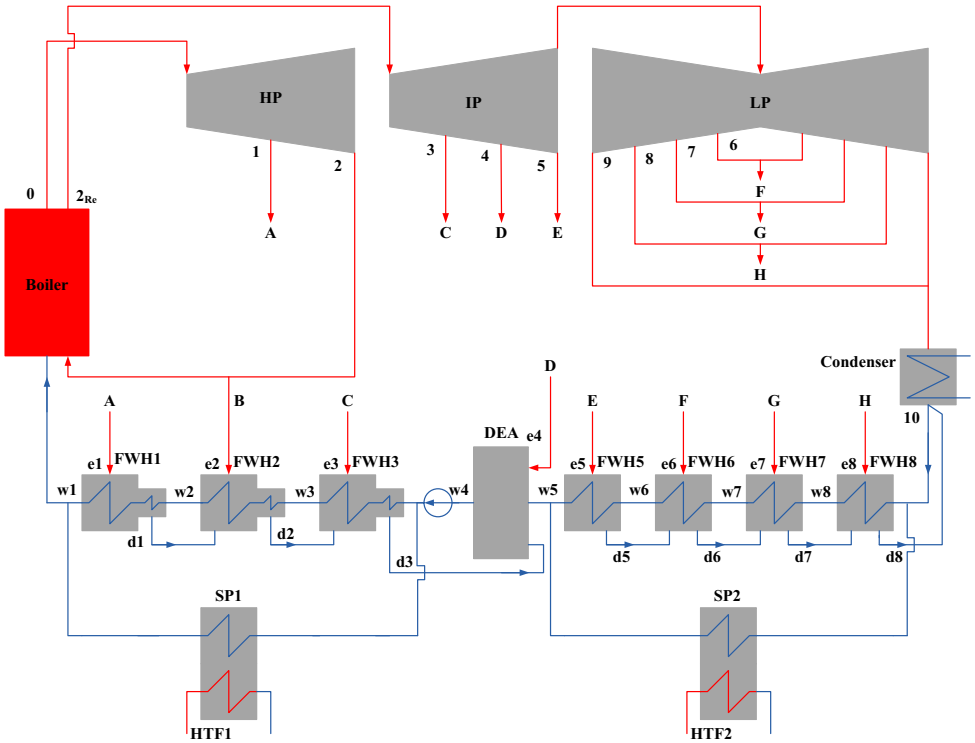

Fig. 2: Schematic diagram of a Parallel 2 (P2) SAPG plant, HTF 1 is used to displace the extraction steam at points A to C and HTF2 is used to displace the extraction steam at points E to H.

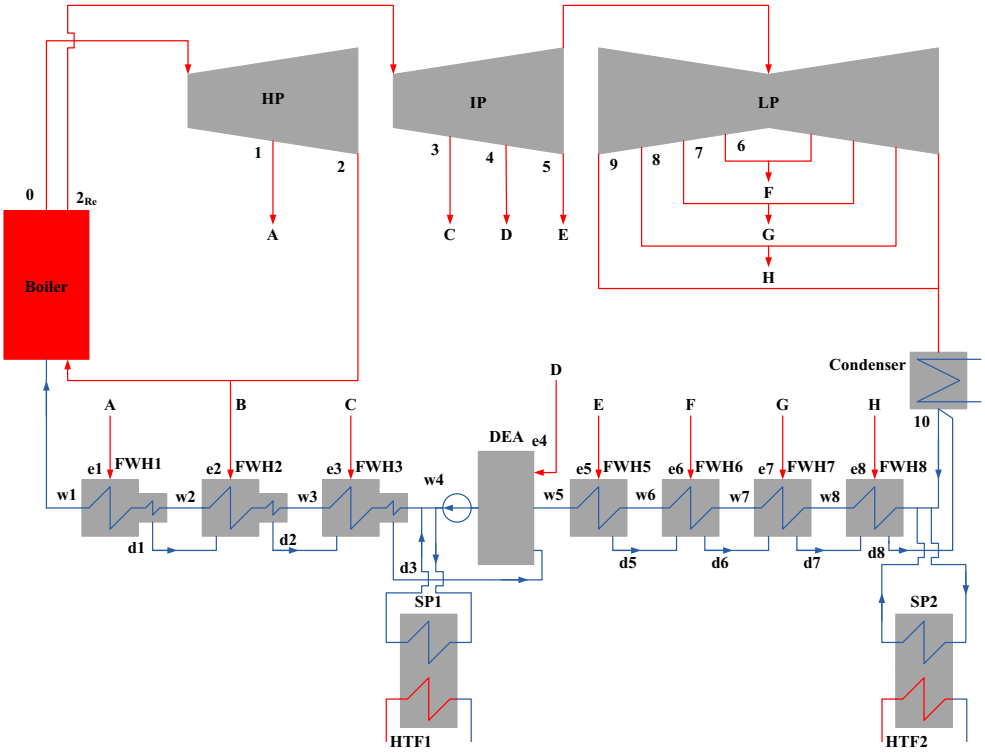

Fig. 3: Schematic diagram of a Series 1 (S1) SAPG plant, HTF 1 is used to displace the extraction steam at points A to C and HTF2 is used to displace the extraction steam at points E to H.

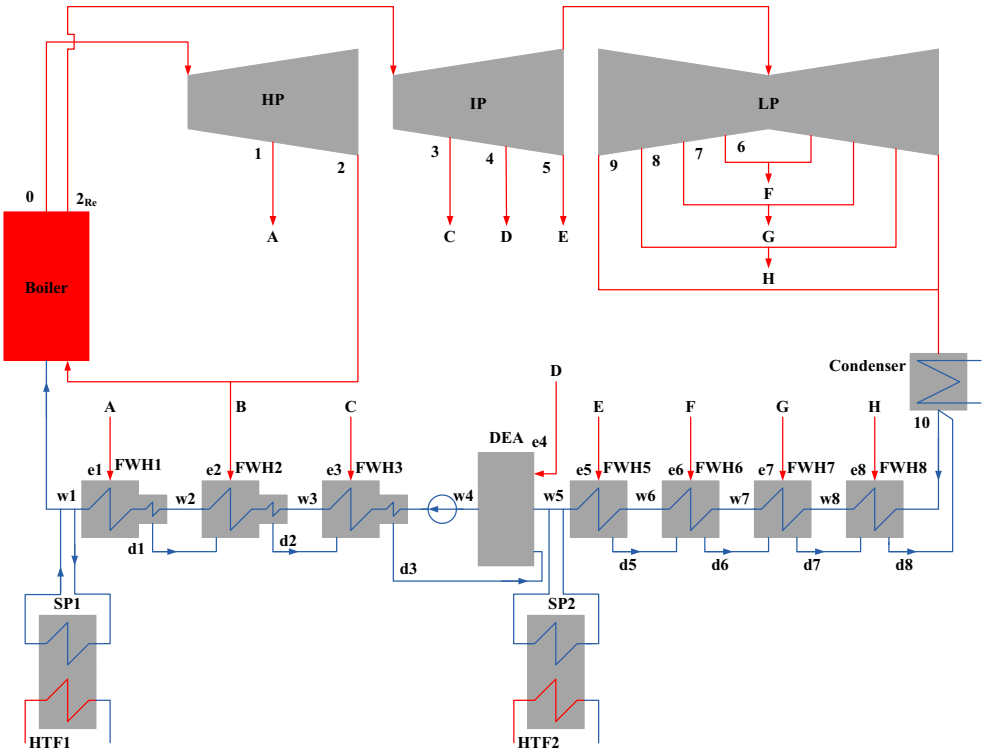

Fig. 4: Schematic diagram of a Series 2 (S2) SAPG plant, HTF 1 is used to displace the extraction steam at points A to C and HTF2 is used to displace the extraction steam at points E to H.

Table 1: Four configurations and their possible control approaches

Configuration	Locations of SPs	Control approach
Parallel 1 (P1)	Parallel with FWH	CT
Parallel 2 (P2)	Parallel with FWH	CT
		HL-VT
		LH-VT
Series 1 (S1)	Series with FWH	CT
Series 2 (S2)	Series with FWH	CT
		HL-VT

3. Methodology

3.1. Pseudo-dynamic model

In order to evaluate the performance of an SAPG plant under variable solar radiation, a pseudo-dynamic model has been developed. The pseudo-dynamic simulation models of four configurations are based on steady state simulation. The steady state simulation model is developed by using the matrix method of an SAPG plant (Hou et al., 2013). The pseudo-dynamic models simulate the technical performance of an SAPG plant at a series of time intervals. At each time interval, the SAPG plant is assumed to be operated at a steady state. A stable mass flow rate of HTF at a constant temperature in each time interval is input into the model.

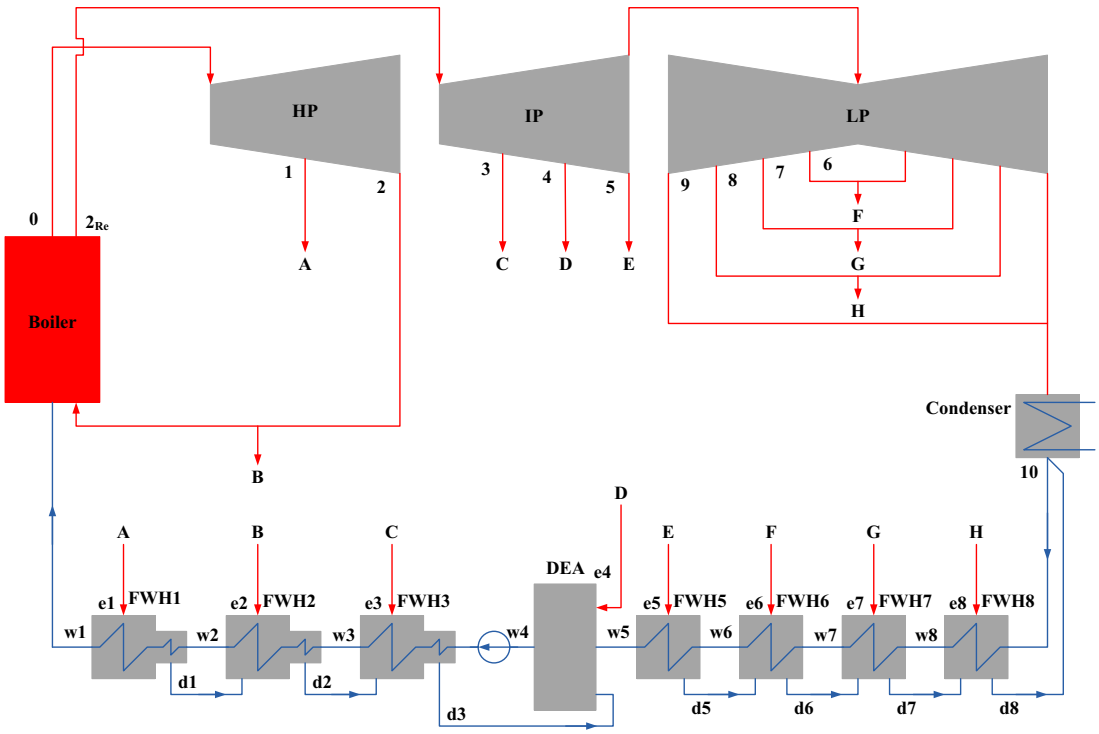

Fig. 5: Schematic diagram of a reference power plant used to demonstrate the matrix method; the power plant has seven closed FWHs and one deaerator (DEA).

Figure 5 shows a reference power plant used to demonstrate the matrix method. As shown, the reference power plant has seven closed FWHs and one deaerator which is an open FWH. In the matrix method, the

simulation is based on the heat and mass balance calculation of the FWH system. The heat and balance equation of the FWH system is given as,

$$\begin{pmatrix} q_1 & \cdots & \cdots & \cdots & \cdots & \cdots & \cdots & 0 \\ r_2 & q_2 & \ddots & \ddots & \ddots & \ddots & \ddots & \vdots \\ r_3 & r_3 & q_3 & \ddots & \ddots & \ddots & \ddots & \vdots \\ r_4 & r_4 & r_4 & q_4 & \ddots & \ddots & \ddots & \vdots \\ \tau_5 & \tau_5 & \tau_5 & \tau_5 & q_5 & \ddots & \ddots & \vdots \\ \tau_6 & \tau_6 & \tau_6 & \tau_6 & \tau_6 & q_6 & \ddots & \vdots \\ \tau_7 & \tau_7 & \tau_7 & \tau_7 & \tau_7 & \tau_7 & q_7 & \vdots \\ \tau_8 & \tau_8 & \tau_8 & \tau_8 & \tau_8 & \tau_8 & \tau_8 & q_8 \end{pmatrix} \cdot \begin{pmatrix} y_A \\ y_B \\ y_C \\ y_D \\ y_E \\ y_F \\ y_G \\ y_H \end{pmatrix} + \begin{pmatrix} \dot{Q}_{Solar,1}/\dot{m}_0 \\ \dot{Q}_{Solar,2}/\dot{m}_0 \\ \dot{Q}_{Solar,3}/\dot{m}_0 \\ 0 \\ \dot{Q}_{Solar,5}/\dot{m}_0 \\ \dot{Q}_{Solar,6}/\dot{m}_0 \\ \dot{Q}_{Solar,7}/\dot{m}_0 \\ \dot{Q}_{Solar,8}/\dot{m}_0 \end{pmatrix} = \begin{pmatrix} \tau_1 \\ \tau_2 \\ \tau_3 \\ \tau_4 \\ \tau_5 \\ \tau_6 \\ \tau_7 \\ \tau_8 \end{pmatrix} \quad \text{(eq.1)}$$

where q_i (kJ/kg) is the specific enthalpy decrease of extraction steam in the ith FWH; τ_i (kJ/kg) is the specific enthalpy increase of the feedwater in the ith FWH; and r_i (kJ/kg) is the specific enthalpy decrease of the drained steam from the (i-1)th FWH in the ith FWH. For the Closed FWHs (FWH 1 to 3 and 5 to 8 in Fig. 5) and the Open FWH (DEA in Fig. 5), the q_i, τ_i and r_i are described as follows:

Closed FWH: $q_i = h_{ei} - h_{di}; \tau_i = h_{fi} - h_{fi+1}; r_i = h_{di-1} - h_{di}$

Open FWH: $q_i = h_{e4} - h_{w5}; \tau_i = h_{w4} - h_{w5}; r_i = h_{d3} - h_{w5}$.

In Eq.1, $y_i (i = A\ to\ H)$ equals the $\dot{m}_i/\dot{m}_0$, and $\dot{m}_i$ (kg/s) is the mass flow rate of extraction steam at each extraction point, $\dot{m}_0$ (kg/s) is the mass flow rate of steam through the boiler (point 0 in Fig. 5).

In order to evaluate the performance of the four configurations of an SAPG plant, the solar power output, and solar power output per solar collector area are calculated.

- Solar power output (W_{Solar}, MW):

$$W_{Solar} = W_{Total} - W_{Ref}, \quad \text{(eq. 2)}$$

where W_{Total} (MW) is the total power output of the power plant after solar input (power boosting purpose), and W_{Ref} (MW) is the output of the power plant without solar input.

- Solar power output per solar collector area (kWh/m^2):

$$x_{Solar} = \frac{W_{Solar}\Delta t}{1000.A_{Solar}}, \quad \text{(eq. 3)}$$

where W_{Solar} (MW) is the solar power output, A_{Solar} (m^2) is the solar collector area.

3.2. Solar resource

In the present paper, historical solar radiation data from 2010 for Adelaide (34ºS, 138ºC) were selected for the evaluation. The historical data were taken from the Australia Government Bureau of Meteorology (BOM, 2014). The solar radiation data for two consecutive five typical days in summer and winter were used for the simulation. Figure 6 and 7 show the hourly solar radiation of consecutive five typical days in summer and winter, respectively.

3.3. Case study

The power plant shown in Fig. 5 is used as case study for comparison. It is a 300MW sub-critical power plant and the solar heat is used to displace the extraction steam at points A to C. In order to displace the extraction steam, it is assumed there is a 10 ºC temperature difference between the feedwater temperature and HTF temperature, so the temperature of HTF from the solar field is at 280 ºC. The solar heat is assumed to be collected by the LS-2 parabolic trough solar collector. The area of each set of LS-2 solar collector is

235.5 m2 (Length 47.1 m, Width 5 m). It is assumed that 200, 300, 400 and 500 sets of LS-2 solar collectors are used to collect solar heat for feedwater preheating purposes. The simulation of the LS-2 solar field is based on the previous work of Zhou et al. (2015).

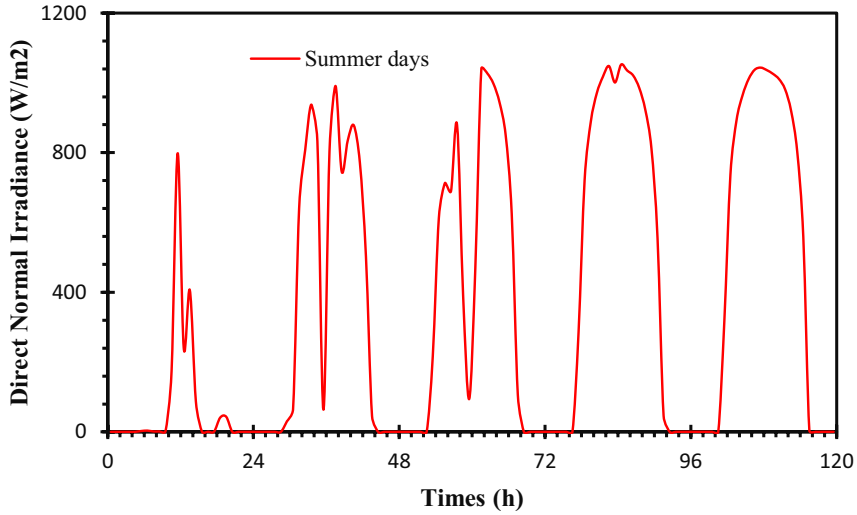

Fig. 6: Hourly Direct Normal Irradiance (W/m², DNI) on five consecutive typical days in summer for Adelaide.

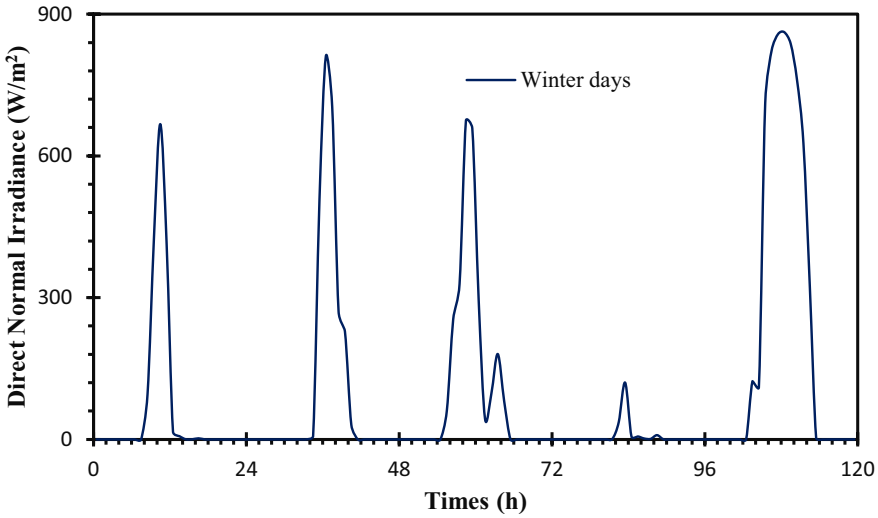

Fig. 7: Hourly Direct Normal Irradiance (W/m², DNI) on five consecutive typical days in winter for Adelaide.

4. Results

Figures 8 and 9 present the hourly solar power ouptut of SAPG plants with different configurations and controlled with different approaches on five consecutive typical days in summer and winter using 500 sets of parabolic trough solar collectors to produce the HTF. As shown in these figures, the P1 configuration and the P2 configuration both controlled in the CT approach have the same hourly solar power output. These two secnarios are the most common SAPG plants of previous works. It is also shown that the P1 configuration controlled in the LH-VT approach and the S1 configuration controlled in the CT approach also have the

same hourly solar power output. The results of Figures 8 to 9 also show that the P2 configuration controlled in the HL-VT approach has the highest hourly solar power output on the days both in summer and winter, and the P1 configuration controlled in the LH-VT approach and the S1 configuration controlled in the CT approach have the lowest hourly solar power output.

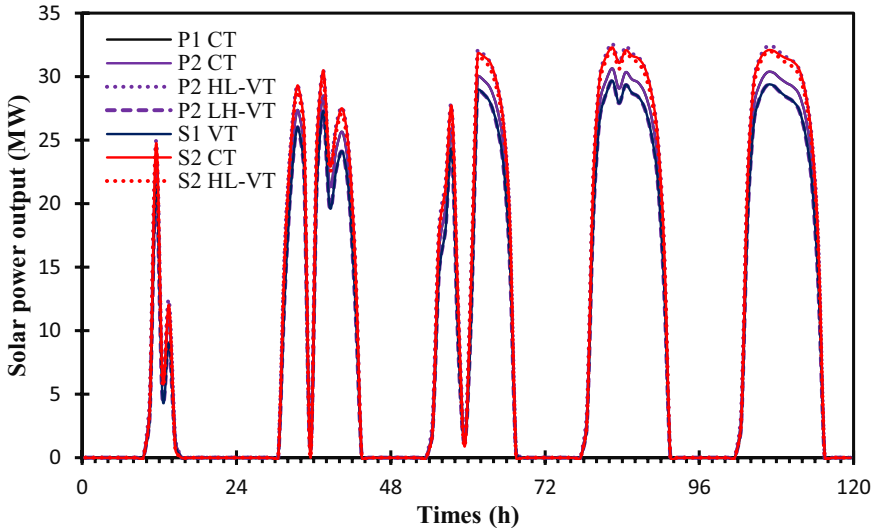

Fig. 8: Hourly solar power output of different configurations controlled with different approaches on five consecutive typical days in summer using 500 sets of parabolic trough solar collectors to produce HTF. P1 and P2 configurations both controlled in the CT approach is the most common SAPG plants of previous works.

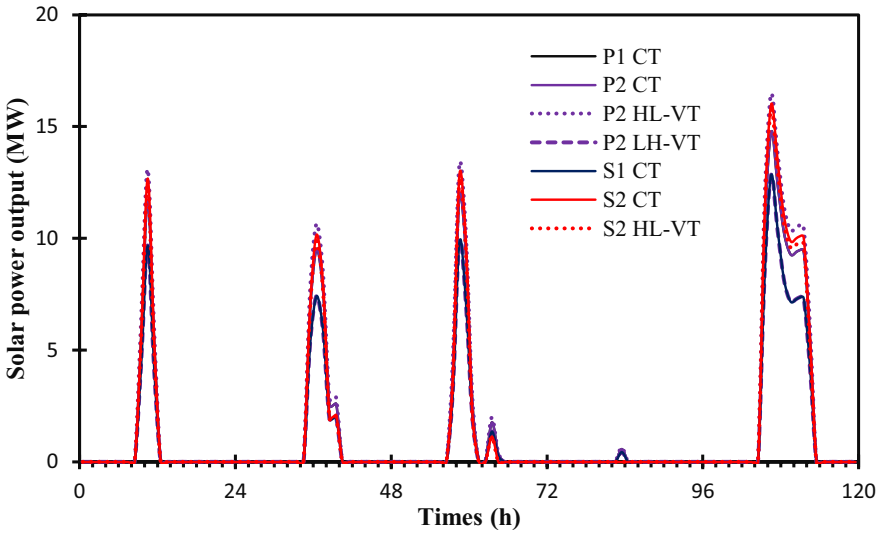

Fig. 9: Hourly solar power output of different configurations controlled with different approaches on five consecutive typical days in winter, using 500 sets of parabolic trough solar collectors to produce HTF. P1 and P2 configurations both controlled in the CT approach is the most common SAPG plants of previous works.

From Fig.8 to 9, it is also shown that the S2 configuration controlled in the CT and HL-VT approach have second and third best hourly solar power ouput. However, in the S2 configuration, the HTF temperature exiting the SP changes with variations in solar radiation. In other configurations, the HTF temperatures exiting the SPs remain constant at 180 ^{o}C, which is lower than in the S2 configuration. This means that the heat loss in the solar collectors of the S2 configuration is higher than the other configurations. Namely, the solar filed efficiency of the S2 configuration is lower than other configurations. Figure 10 and Figure 11

show the HTF temperature exiting the SP on five consecutive days in the summer and winter, respectively. It is shown that the S2 configuration controlled in the VT-HL appraoch have higher HTF temperature exiting SP than the S2 configuration controlled in the CT appraoch. This means that the heat loss in the solar collector of the S2 configuration controlled in the VT-HL appraoch is higher than the S2 configuration controlled in the CT appraoch.

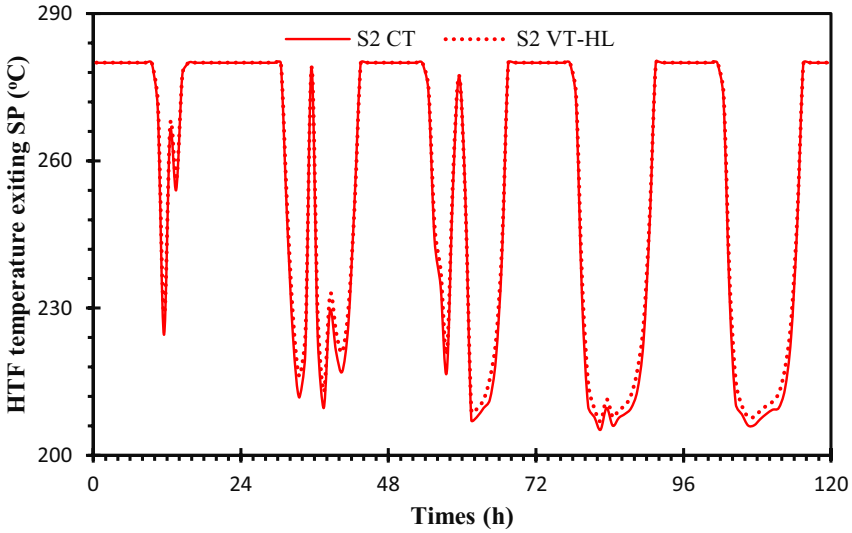

Fig. 10: HTF temperature exiting SP (°C) for S2 configuration controlled in CT and HL-VT approach on five consecutive typical days in summer, using 500 sets of parabolic trough solar collectors to produce HTF.

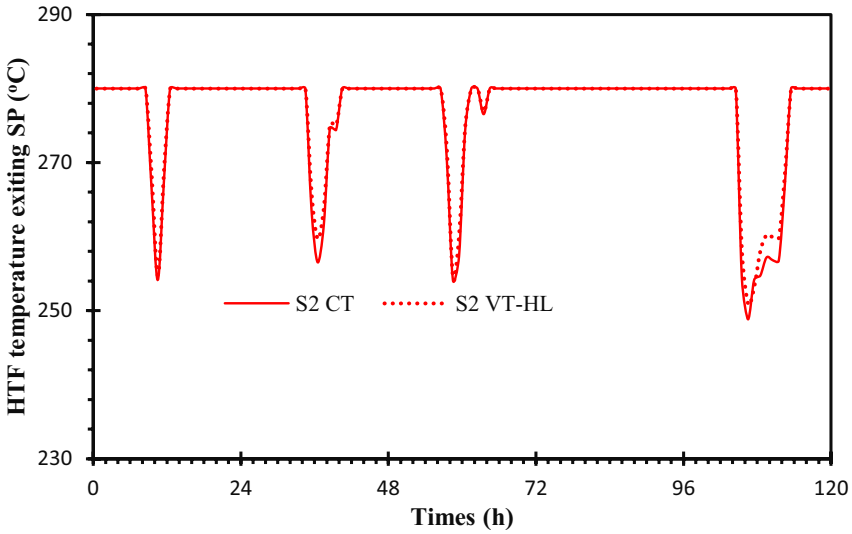

Fig. 11: HTF temperature exiting SP (°C) for S2 configuration controlled in CT and HL-VT approach on five consecutive typical days in winter, using 500 sets of parabolic trough solar collectors to produce HTF.

Figures 12 to 13 present the daily solar power output per solar collector area (x_{Solar}) for the SAPG plant with different configurations on five consecutive typical days in summer and winter, respectively. It is shown in Figures 12 and 13 that the P2 configuration controlled in the HL-VT approach have the maximum x_{Solar} in both summer and winter days. This is caused by the highest hourly solar power output. From Figures 12 and 13, the results indicate that for the S1 consifugration controlled in the CT appraoch and P1 configuration controlled in the LH-VT approach, the x_{Solar} increases with the incremental solar collector area. The reason is thought to be cuased by the larger solar collector area means more solar thermal energy used for

displacement purpose, which means more high quality (higher pressure extraction steam) extraction steam is dispalced. In contrast, for the other cases, the x_{Solar} decreases with the incremental solar collector area.

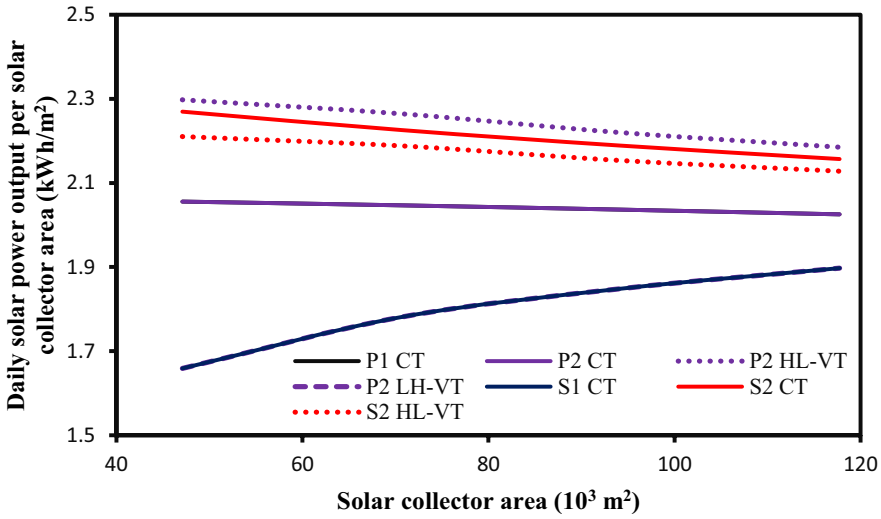

Fig. 12: Daily solar power output per solar collector area (x_{Solar}, kWh/m²) on five consecutive days in summer.

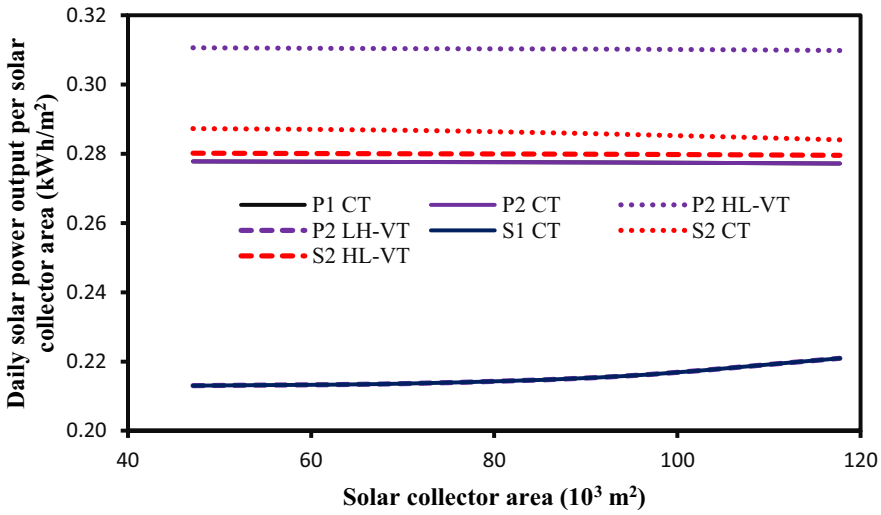

Fig. 13: Daily solar power output per solar collector area (x_{Solar}, kWh/m²) on five consecutive days in summer.

Tab. 4: Ratio of power output on five consecutive days in summer to that in winter

No. of collector sets	P1CT	P2CT	P2HL-VT	P2LH-VT	S1CT	S2CT	S2VT-HL
200	7.40	7.40	7.40	7.79	7.79	7.90	7.89
300	7.37	7.37	7.30	8.34	8.34	7.76	7.82
400	7.34	7.34	7.16	8.57	8.57	7.66	7.70
500	7.31	7.31	7.05	8.59	8.59	7.59	7.61

Table 4 presents the ratio of power output on five consecutive days in summer to that in winter ($W_{Solar}\Delta t_{Summer}/W_{Solar}\Delta t_{Winter}$). The higher $W_{Solar}\Delta t_{Summer}/W_{Solar}\Delta t_{Winter}$ means the higher impact of variations in solar radiation on SAPG's performance. It is shown that the P2 configuration controlled in the HL-VT appraoch has the lowest $W_{Solar}\Delta t_{Summer}/W_{Solar}\Delta t_{Winter}$. This means that variatios in solar radiation have the lowest impact on the performacne of P2 configuration controlled in the HL-VT approach. It is also shown that for the P2 configuration controlled in the LH-VT approach and S1 configuration, $W_{Solar}\Delta t_{Summer}/W_{Solar}\Delta t_{Winter}$ increases with the incremental solar collector area. In contrast, for other cases, $W_{Solar}\Delta t_{Summer}/W_{Solar}\Delta t_{Winter}$ decreases with the incremental solar collector area. This means that for the P2 configuration controlled in the LH-VT approach and S1 configuration, the impact of variatios in solar radiation on the SAPG's performance increases with the incremental solar collector area, while for other cases, the impact of variations in solar radiation decreases with the incremental solar collector area.

5. Conclusions

Pseudo-dynamic simulation models of four possible configurations of the SAPG plant, together with three alternative control strategies for the power boosting operation mode have been developed. The dynamic performances of different SAPG plants have been analysed using hourly solar radiation data in 5 consecutive summer and winter days in a location (Adelaide, Australia), respectively. The total solar power output of the SAPG plant and the daily solar power output per unit solar collector area ($\boldsymbol{x_{Solar}}$) were used as criteria to analyze the dynamic performance of SAPG plants with different configurations and control approaches. The results show that:

- the P2 configuration controlled in the HL-VT approach has the highest hourly solar power output, while the P2 configuration controlled in the LH-VT approach and the S1 configuration controlled in the CT approach have the lowest hourly solar power output in both winter and summer;
- For the S2 configuration, the HTF temperature exiting the SP is higher than other configurations. This indicates that the heat loss in the solar collectors of the S2 configuration is higher than the other configurations;
- The P2 configuration controlled in the HL-VT approach has the highest $\boldsymbol{x_{Solar}}$ in both summer and winter days;
- The variations in solar radiation have the lowest impact on the performance of P2 configuration controlled in the HL-VT approach while have the highest impact on the P1 configuration controlled in the LH-VT approach and the S1 configuration controlled in the CT approach;
- The P2 configuration controlled in the HL-VT approach is the best among the seven configurations and control approaches combinations in the selected location (Adelaide, Australia).

6. References

Australian Government Bureau of Meteorology (BOM), 2014. One minute solar data. http://reg.bom.gov.au/climate/reg/oneminsolar/.

Hu, E., Yang, Y.P., Nishimura, A., Yilmaz, F., Kouzani, A., 2010. Solar thermal aided power generation. Applied Energy. 87, 2881-2885.

Hou, H.J., Yu, Z.Y, Yang, Y.P., Chen, S., Luo, N., Wu, J.J., 2013. Performance evaluation of solar aided feedwater heating of coal-fired power generation (SAFHCPG) system under different operating conditions. 112, 710-718.

Hou, H.J., Wu, J.J., Yang, Y.P., Hu, E., Chen, S., 2015. Performance of a solar aided power plant in fuel saving mode. Applied Energy. http://dx.doi.org/10.1016/j.apenergy.2015.01.092.

Peng, S., Hong, H., Jin, H.G., Zhang, Z.N., 2013. A new rotatable-axis tracking solar parabolic-trough collector for solar-hybrid coal-fired power plants. Solar Energy. 98, 492-502.

Peng, S., Hong, H., Wang, Y.J., Wang, Z.G., Jin, H.G., 2014. Off-design thermodynamic performances on typical days of a 330 MW solar aided coal-fired power plant in China. Applied Energy. 130, 500-509.

Peng, S., Wang, Z.G., Hong, H., Xu, X., Jin, H.G., 2014. Exergy evaluation of a typical 330 MW solar-hybrid coal-fired power plant in China. Energy Conversion and Management. 85, 848-855.

Wu, J.J., Hou, H.J., Yang, Y.P., Hu, E., 2015. Annual performance of a solar aided coal-fired power generation system (SACPG) with various solar field areas and thermal energy storage capacity. Applied Energy. 157, 123-133.

Yan, Q., Yang, Y.P., Nishimura, A., Kouzani, A., Hu, E., 2010. Multi-point and Multi-level Solar Integration into a Conventional Coal-Fired Power Plant. Energy & Fuels. 24, 3733-3738.

Yang, Y.P., Yan, Q., Zhai, R.R., Kouzani, A., Hu, E., 2011. An efficient way to use medium-or-low temperature solar heat for power generation-integration into conventional power plant. Applied Thermal Engineering. 31, 157-162.

Zhou, L.Y., Li, Y.Y., Hu, E., Qin, J.Y., Yang, Y.P., 2015, Comparison in net solar efficiency between the use of concentrating and non-concentrating solar collectors in solar aided power generation systems. Applied Thermal Engineering. 75, 685-691.